

## The removal optimization of Reactive Red X-3B through UV photocatalysis based on the response surface methodology

Shuqin Li, Sinuo Lin, Di Zhang\*, Fan Bu

College of Resources and Environment, Northeast Agricultural University, Harbin, Heilongjiang 150030, China, Tel. 086+45155191170; Fax: 086+45155191170; emails: zhangdi6283@qq.com (D. Zhang), 602311518@qq.com (S. Li), 214752775@qq.com (S. Lin), 1391667067@qq.com (F. Bu)

Received 25 April 2020; Accepted 17 November 2020

### ABSTRACT

The response surface methodology (RSM) was applied to optimize UV photocatalytic reaction conditions treating high-concentration Reactive Red X-3B. The molecular sieve F was made of fly ash by the hydrothermal synthesis method. The molecular sieve loaded nano-TiO<sub>2</sub> (Ti/F) was synthesized with the ion-exchange method. The molecular sieve F and Ti/F were the photocatalysts and its catalyst characteristics were analyzed by using scanning electron microscopy-energy-dispersive X-ray spectroscopy and Brunauer–Emmett–Teller-surface area. The effects of four operating variables, initial dye concentration, photocatalyst dosage, temperature and H<sub>2</sub>O<sub>2</sub> concentration on the decolorization efficiency of Reactive Red X-3B were optimized by RSM based on Box–Behnken design. The pseudo-first-order model could fit the photocatalysis kinetic data well at 20°C. And the pseudo-second-order model could fit the photocatalysis kinetic data well at 40°C. Analysis of variance indicated that the proposed quadratic model could be used to navigate the design space. The maximum removal rate of Reactive Red X-3B was 97.83% when the following optimum conditions were used: Ti/F dosage of 0.80 g/L, H<sub>2</sub>O<sub>2</sub> dosage of 2.01 ml/L, the temperature of 32.5°C, and initial Reactive Red X-3B concentration of 1,824 mg/L. In the regeneration experiments, the removal rate of Reactive Red X-3B gradually decreased with increasing the number of photocatalytic cycles. The regeneration experiments indicated that Ti/F was stable and reusable. The molecular sieve Ti/F could be used as an effective and economical photocatalyst in the removal of Reactive Red X-3B. Maybe the study can be applied in future engineering practice.

*Keywords:* TiO<sub>2</sub>; Reactive Red X-3B; Photocatalysis; Response surface methodology

### 1. Introduction

Dyes are widely used in the textile, printing, leather, and gasoline industries. The wastewater with dark color, strong alkaline, and complex composition from these industries pollutes surface water [1], groundwater [2], and even soils through irrigation [3,4]. Reactive Red X-3B is an azo dye. Due to the toxicity and slow degradation, the azo dyes are classified as environmentally hazardous materials. Every year, more than 80,000 tons of azo dyes

are consumed. A large amount of harmful wastewater is produced. These dyes are the major cause of both surface and groundwater bodies contamination because of their carcinogenicity and toxicity to aquatic life [5–7]. Therefore, azo dyes should be removed from wastewater before it is discharged into water bodies [8].

Photocatalytic oxidation is an effective technology for removing azo dyes from water because it seems like an important “environmentally friendly technology” [9,10]. Nano-TiO<sub>2</sub> photocatalyst is widely used in a variety of

\* Corresponding author.

applications and products in azo dyes wastewater purification systems [11,12]. However,  $\text{TiO}_2$  has some challenges, such as high cost, poor separation performance and hard recovery [13–15]. The development of new materials loaded nano- $\text{TiO}_2$ , therefore, is strongly required to provide enhanced performances with respect to the photocatalytic properties. An intensive study has been carried out to immobilize the  $\text{TiO}_2$  photocatalyst on various supporting materials, such as silica [16,17], montmorillonite [18], zeolites [19,20] and activated carbon [21–24]. The reaction conditions for photocatalytic degradation of organics are important [25]. Usually, the single factor test method is used to figure out the best conditions [26]. The results could only show the single optimal conditions. However, the results on the single factor test are slightly different from the actual ones because the various factors had interactions. In order to optimize the value of effective parameters with the minimum number of experiments, central composite design – the most widely used form of response surface methodology (RSM) – was employed to find improved or optimal process settings in efficient use of the experimental data. Using RSM, it is possible to estimate linear, interaction, and quadratic effects of the factors and to provide a prediction model for the response [27–29]. This method has been used for modeling and optimization of the decolorization process by advanced oxidation processes [30–32]. However, to the best of our knowledge, decolorization of organic dye solutions under Ti/F UV photocatalytic and the effect of the interaction of effective parameters using central composite design have not been studied [33,34]. In this work, the central composite design has been applied to the modeling and optimization of decolorization of dye solutions containing Reactive Red X-3B by Ti/F UV photocatalytic have been studied. The influencing factors (variables) investigated were initial dye concentration, photocatalyst dosage, temperature and  $\text{H}_2\text{O}_2$  concentration and decolorization efficiency was monitored as the process response. Counter plots and response surfaces were drawn to predict the efficiency of the decolorization process under different values of the independent parameters [35–37].

## 2. Materials and methods

### 2.1. Materials

Fly ash was purchased from Jixi Datang Second Heating Co. as a crude material to produce the molecular sieve.  $\text{TiO}_2$  (99.8 wt.%) was obtained from Maikun Chemical Reagent Co., Ltd. Reactive Red X-3B was supplied by Xinxing Chemical Dyestuff Co., Ltd. Hydrochloric acid (HCl, 37 wt.%) was from Xilong Chemical Co., Ltd. Sodium hydroxide (NaOH), hydrogen peroxide ( $\text{H}_2\text{O}_2$ , 30 wt.%) and anhydrous ethanol ( $\text{CH}_3\text{CH}_2\text{OH}$ , 99.7 wt.%) were obtained from Tianjin Hengxing Reagent Co. All the chemicals were used without further purification.

#### 2.1.1. Preparation of molecular sieve F

Molecular sieve F was synthesized by a hydrothermal process utilizing fly ash. First, the fly ash was sieved using a 40-mesh stainless steel sieve. The sieved fly ash and the 50% HCl were mixed in 100 mL of the beaker, followed by

vigorous stirring at 80°C for 2 h. The molar rate ratio of fly ash: HCl in the mixture was 1:1. Subsequently, the mixed liquor was rinsed several times with anhydrous ethanol to be neutral and then dried at 80°C. After that, the dry solid was mixed with NaOH according to the mass ratio of 1.3:1 and then calcined at 600°C for 12 h. Then, the powder was added to deionized water (10 ml water for 1 g sample at every turn) and stirred magnetically for 12 h. At last, the mixed solution was loaded into a hydrothermal reactor and crystallized at 90°C for 24 h. The material was adjusted to reach near-neutral pH. Then, the prepared sample was dried at 90°C for 12 h and used as molecular sieve F.

#### 2.1.2. Preparation of molecular sieve Ti/F

First, the  $\text{TiO}_2$  and F were mixed in ethanol (10% by weight) to obtain a homogeneous solution. Subsequently, the solution was stirred magnetically at 95°C for 3 h. Last, the Ti/F was obtained after calcining at 550°C for 3 h. The Ti/F was used as a photocatalyst. The ultimate analyses of the molecular sieves F and Ti/F were presented in Table 1 and Fig. 1. The Ti/F habited the high recyclable performance was shown in supporting information. The scanning electron microscopy-energy-dispersive X-ray spectroscopy of that molecular sieve F and Ti/F have been analyzed (S1). And the results showed Ti/F was stable and reusable (S4).

## 2.2. Experimental design

### 2.2.1. Kinetics of Reactive Red X-3B on F and Ti/F

For the kinetic experiments, 0.050 g catalysts and 100  $\mu\text{L}$   $\text{H}_2\text{O}_2$  solution were added into 50 mL Reactive Red X-3B solution with an initial concentration of 2000 mg/L and  $\text{pH} = 7.0 \pm 0.2$  at 20°C or 40°C. Simultaneously, the two control groups were used: with photocatalyst and without photocatalyst. Aliquots of the solution were withdrawn at various time intervals (0–600 min) for further analysis. In addition, the kinetic model was used to simulate the Reactive Red X-3B photocatalytic process, which could be expressed as Eqs. (1) and (2):

*Pseudo-first-order kinetic equation:*

$$\ln\left(\frac{C_t}{C_0}\right) = -k_1 t \quad (1)$$

*Pseudo-second-order kinetic equation:*

$$\frac{t}{(C_0 - C_t)} = \frac{1}{\left[k_2(C_0 - C_e)^2\right]} + \frac{t}{(C_0 - C_e)} \quad (2)$$

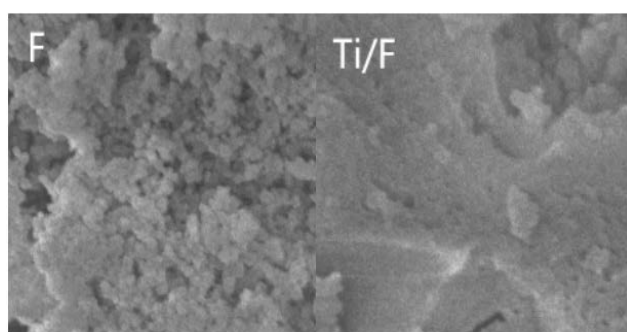
where  $C_t$  (mg/L) was the concentration of Reactive Red X-3B at any time  $t$  (min);  $C_0$  (mg/L) was the initial concentration of Reactive Red X-3B;  $C_e$  (mg/L) was the balanced concentration of Reactive Red X-3B;  $k$  was the kinetic constant.

### 2.2.2. RSM test design

The aim of the study was to explore the most significant variables of optimal conditions for UV photocatalytic

Table 1  
Characteristics of the surface properties of molecular sieve F and Ti/F

Surface properties	F	Ti/F
Brunauer–Emmett–Teller single point surface area (m <sup>2</sup> /g)	24.11	10.91
Brunauer–Emmett–Teller multiple point surface area (m <sup>2</sup> /g)	23.28	10.44
Langmuir surface area (m <sup>2</sup> /g)	37.92	17.41
T-plot micropore surface area (m <sup>2</sup> /g)	2.99	0.24
T-plot surface area (m <sup>2</sup> /g)	21.13	10.67
Pore volume ( $P/P_0 = 0.9919$ ; pore diameter < 240.4 nm) (mL/g)	160.3	76.5
T-plot micropore volume (mL/g)	1.42	0.11
Average pore diameter (4V/A by Brunauer–Emmett–Teller, nm)	26.59	28.04



Element		C	O	Na	Al	Si	K	Ti	Ca	Fe	Cu	Mg
F	Weight ratio	12.52	47.62	7.82	9.29	18.83	1.25	1.19	0.47	0.95	0.06	-
	Atomicity ratio	19.08	54.52	6.23	6.31	12.28	0.59	0.45	0.22	0.31	0.02	-
Ti/F	Weight ratio	12.71	49.18	7.88	9.06	17.29	0.96	1.5	0.36	0.74	-	0.32
	Atomicity ratio	19.18	55.71	6.21	6.09	11.16	0.44	0.57	0.16	0.24	-	0.24

Fig. 1. Scanning electron microscopy-energy-dispersive X-ray spectroscopy of F and Ti/F.

reaction. The key factors for the removal rate of Reactive Red X-3B were molecular sieve, photocatalyst dosage, the dosage of H<sub>2</sub>O<sub>2</sub>, substrate concentration, and the reaction temperature, of which the molecular sieve was the most important variable. Two different molecular sieves were chosen to represent the different catalysts used in the photocatalytic reaction. To explore the effect of photocatalyst dosage, H<sub>2</sub>O<sub>2</sub> dosage, substrate concentration, and reaction temperature, the removal rate was employed (Table 2). The range of the photocatalyst dosage was 0.5–1.5 g/L, the dosage of H<sub>2</sub>O<sub>2</sub> was 1–3 ml/L, the dosage of the substrate concentration was 1,500–2,500 mg/L, and the range of temperature was 20°C–40°C. The settings for the process variables were chosen based on optimal values obtained for the single factor test (S3). The model was taken into account the linear equation, the 2FI, the quadratic and the cubic effects of catalyst dosage (*A*), substrate concentration (*B*), H<sub>2</sub>O<sub>2</sub> dosage (*C*), and temperature (*D*). Each model was evaluated based on R<sup>2</sup>, *p*-value, *F*-value, and relative squared error. The significance of each parameter was evaluated based on *p*-values. RSM was used to evaluate the effect of each parameter based

Table 2  
Factor levels for the experimental design

Code value	-1	0	1
Photocatalyst dosage (g/L)	0.5	1.0	1.5
H <sub>2</sub> O <sub>2</sub> dosage (ml/L)	1.0	2.0	3.0
Substrate concentration (mg/L)	1,500	2,000	2,500
Temperature (°C)	20	30	40

on statistically significant coefficients. The experiment was designed by four factors and three levels. All other experiments were performed three times in duplicates.

### 2.2.3. Photocatalytic experiment

The photocatalytic degradation experiments for dye removals were performed by UV irradiation with an intensity of 5.5 mW/cm<sup>2</sup> (254 nm, HL100CH-5 lamp, SEN LIGHTS Co., Osaka, Japan) or by simulated solar irradiation (Shanghai Xinweng Scientific Instrument Co., Ltd.) (S2). The reactor system included a cylindrical PYREX-glass cell with a working volume of 1.0 L and a lamp (mercury light, 1,000 W) placed in a 50 mm diameter quartz tube. The working temperature of the reactor was kept unchanged around 20°C by a circulated cooling water system. A certain amount of F and Ti/F was placed respectively in 50 ml Reactive Red X-3B solution with some volume 30% H<sub>2</sub>O<sub>2</sub>. All samples were placed in a 50 ml quartz tube and irradiated by UV for 630 min. The samples (5 ml) were taken out and filtered with a 0.45 μm syringe membrane filter to completely remove suspended photocatalysts at a preset time. Every sample was measured in triplicate and averaged. The absorption spectrum and a molecular formula of Reactive Red X-3B are shown in Fig. 2. The concentrations of Reactive Red X-3B in the samples were measured at maximum wavelengths ( $\lambda_{max}$ ) of 535 nm on a JASCO V650 spectrophotometer. The removal rates ( $\eta$ ) were calculated according to the following equations.

$$\eta = \frac{C_0 - C_i}{C_0} \times 100\% \quad (3)$$

where  $C_0$  and  $C_i$  were the dye concentrations at the initial time and time *i*, respectively.

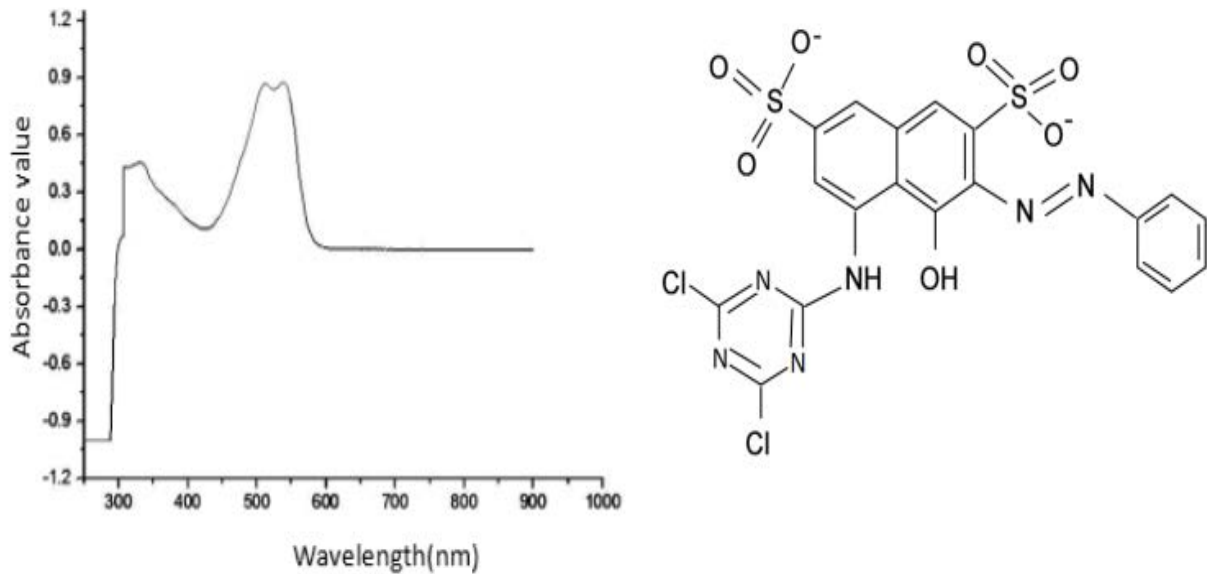


Fig. 2. (a) Absorption spectrum and (b) molecular formula of Reactive Red X-3B.

### 3. Results and discussion

#### 3.1. Photocatalytic kinetic study of F and Ti/F

Some dyes are degraded by direct UV radiation. Therefore, it should be examined to what extent the Reactive Red X-3B are 'photolyzed' if no catalyst was used. Blank experiments (CK) were carried out for the dye without a catalyst for this purpose. A significantly increased removal rate was observed at 40°C compared with 20°C. A similar trend was observed in UV radiation treatments. Therefore, the temperature has been proved to be an important aspect (shown in Fig. 3). Although the semiconductor photocatalysis is usually not very temperature-dependent, an increase in temperature helped the reaction to compete more efficiently with recombination and causes an increase in removal reaction rate.

The Reactive Red X-3B can be adsorbed by molecular sieves without UV radiation. F and Ti/F (1 g/L) treatments were carried out for the determination of adsorption kinetics. The content of adsorption was similar in the two groups and ranged from 1.59% to 4.24%. The percent of degradation increased on F and Ti/F increased first rapidly with an increase. The equilibrium time (about 300 min) of F and Ti/F at 40°C were faster than that (about 600 min) at 20°C. A significant effect on the photocatalytic capacity of Ti/F was higher than F in the first 30 min especially.

As indicated in Table 3, the pseudo-first-order kinetic model could better describe the photocatalytic process of Reactive Red X-3B by the catalyst, compared with the pseudo-second-order kinetic model at 20°C. The  $R^2$  values of F and Ti/F were 0.9934 and 0.9591 fitted with the pseudo-first-order kinetics. The  $R^2$  values of the pseudo-second-order kinetic model at 40°C were 0.9741 and

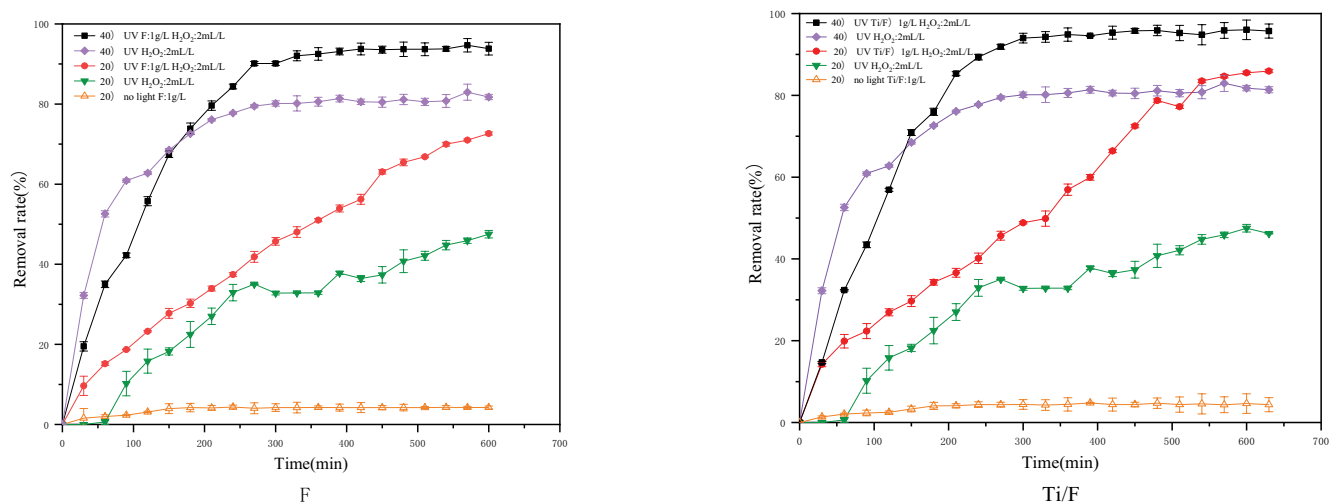


Fig. 3. Effect of time on Reactive Red X-3B degradation on (a) F and (b) Ti/F.

Table 3  
Kinetic constant for the modelling process

Temperature	Kinetic	F		Ti/F	
		<i>k</i>	<i>R</i> <sup>2</sup>	<i>k</i>	<i>R</i> <sup>2</sup>
20°C	Pseudo-first-order kinetic	0.00221	0.9934	0.00330	0.9591
	Pseudo-second-order kinetic	0.00226	0.7621	0.00189	0.6807
40°C	Pseudo-first-order kinetic	0.00490	0.8494	0.00555	0.8341
	Pseudo-second-order kinetic	0.01003	0.9741	0.00865	0.9568

0.9568. Those results were implied that the photocatalytic process of Reactive Red X-3B onto catalyst was suitable for the pseudo-second-order kinetic model. A similar conclusion had been reported by Deng et al. [38] about the pseudo-second equation, which can better describe the Reactive Red X-3B adsorption procedure on TiO<sub>2</sub>/Al<sub>2</sub>O<sub>3</sub>.

### 3.2. Response surfaces model fitting of molecular sieve F

Response surfaces model was used to fit the results of photocatalysis of molecular sieve F by Box–Behnken experimental design. The statistical analysis for F of response surfaces model fitting is seen in Tables 4 and 5. It was shown that the “Pred. *R*-Squared” of the quadratic model was closest to 1, the “Sequential *p*-value” was less than 0.0001, and its “lack of fit *p*-value” was greater than 0.05. The results implied that the removal rates of Reactive Red X-3B by molecular sieve F were fitted to the following quadratic model:

$$R_1 = 94.27 + 1.71A - 22.21B + 7.87C + 6.10D - 3.05AB + 7.83AC - 7.90AD - 5.61BC + 0.75BD + 5.42CD - 9.90A^2 - 17.95B^2 - 23.01C^2 - 14.6D^2 \quad (4)$$

where *R*<sub>1</sub>: removal rate (%); *A*: code value of catalyst dosage; *B*: code value of substrate concentration; *C*: code value of H<sub>2</sub>O<sub>2</sub> dosage; *D*: code value of temperature.

As the results in Table 4 show, the “lack of fit” of 0.0836 was indicated that the model terms were significant. Therefore, the model could be navigated. Kumar et al. [39] had found that the value of “*R*-Squared” was closer to the one, which process of nanocomposite for enhanced dye-sequestration was fitting the linear model.

The effects of photocatalyst dosage, the dosage of H<sub>2</sub>O<sub>2</sub>, substrate concentration, and temperature on the removal rate of Reactive Red X-3B based on the single factor test were significant (S3). The single factor test results showed

that the higher temperature promoted the degradation of Reactive Red X-3B. The removal rate was increased with the temperature from 20°C to 30°C; however, the removal rate essentially unchanged at above 30°C. The effect of increasing photocatalyst F dosage on removal rate was not obvious. However, the RSM plot of temperature and catalyst dosage reflected the strong interaction (Fig. 4a). Response surface contour method was used to analyze the interaction between temperature and catalyst dosage on the photocatalytic reaction of Reactive Red X-3B. Minima removal rate was obtained with the temperature of 20°C–21.3°C and the catalyst dosage was from 0.5 to 0.63 g/L. When the temperature raised to 38.2°C, the removal rate increased rapidly to 94% with catalyst dosage increasing. Therefore, the catalyst dosage increased to 1.18 g/L and the removal rate had decreased. Similarly, the removal rate had a little change and then decreased slightly with the catalyst dosage increased in 38.2°C–40°C. When the temperature was constant, the range of five tangent points for different contour lines and catalyst dosage variation horizontal lines was 0.86–1.18 g/L. Also, the removal rate gradually increased and then tended to remain unchanged as the temperature increased, while the catalyst dosage was 0.5–0.63 g/L. Similarly, when the temperature increasing, the removal rate increased first with a maximum value of 94% and then decreased by increasing catalyst dosage from 0.63 to 1.5 g/L. When the catalyst dosage was constant, the four tangent points of the different contour lines and perpendicular lines of temperature were in the range of 30°C–34°C. It was included that the interaction between the temperature and the catalyst dosage was obvious with the large extreme point deviation. When the catalyst dosage was 0.98–1.10 g/L and the temperature was 30°C–33.7°C or catalyst dosage was 0.86–1.06 g/L and the temperature was 31.5°C–34°C, the removal rate of Reactive Red X-3B (2,000 mg/L) was 94%.

The H<sub>2</sub>O<sub>2</sub> dosage showed a less pronounced effect on the removal rate than the temperature. The H<sub>2</sub>O<sub>2</sub> dosage

Table 4  
Statistical analysis for F of response surface model fitting

Source	Sequential <i>p</i> -value	Lack of fit <i>p</i> -value	Adj. <i>R</i> -Squared	Pred. <i>R</i> -Squared
Linear	0.0006	<0.0001	0.4689	0.4252
2FI	0.836	<0.0001	0.3841	0.3155
Quadratic	<0.0001	0.0836	0.9969	0.9917
Cubic	0.0337	0.4013	0.9991	0.9892

Table 5  
Variance analysis of Box–Behnken experimental design

Source	Sum of squares	df	Mean square	F-value	p-value Prob. > F	Significance analysis
Model	13,091.04	14	935.07	653.03	<0.0001	Significant
A	34.95	1	34.95	24.41	0.0002	
B	5,917.63	1	5,917.63	4,132.74	<0.0001	
C	743.87	1	743.87	519.5	<0.0001	
D	446.03	1	446.03	311.5	<0.0001	
AB	37.09	1	37.09	25.9	0.0002	
AC	245.08	1	245.08	171.16	<0.0001	
AD	249.48	1	249.48	174.23	<0.0001	
BC	126.11	1	126.11	88.07	<0.0001	
BD	2.22	1	2.22	1.55	0.2335	
CD	117.61	1	117.61	82.14	<0.0001	
A <sup>2</sup>	635.62	1	635.62	443.9	<0.0001	
B <sup>2</sup>	2,090.91	1	2,090.91	1,460.25	<0.0001	
C <sup>2</sup>	3,435.55	1	3,435.55	2,399.31	<0.0001	
D <sup>2</sup>	1,389.6	1	1,389.6	970.46	<0.0001	
Residual	20.05	14	1.43			
Lack of fit	18.37	10	1.84	4.38	0.0836	Not significant
Pure error	1.68	4	0.42			
Cor. total	13,111.09	28				

above 2 ml/L may simply lead to Reactive Red X-3B degradation being inhibited. A small though the positive effect was seen from H<sub>2</sub>O<sub>2</sub> dosage under 2 ml/L. Furthermore, H<sub>2</sub>O<sub>2</sub> dosage had a significantly positive and negative interaction on the reaction. The results indicated that the removal rate was further changed with simultaneous small or large parameter values. However, the effects and the strong interaction with H<sub>2</sub>O<sub>2</sub> dosage dominated the RSM plot of H<sub>2</sub>O<sub>2</sub> dosage and catalyst dosage (Fig. 4b). The removal rate had increased to the maximum and then decreased with increasing H<sub>2</sub>O<sub>2</sub> dosage, while catalyst dosage was constant. The four tangent points of different contour lines and H<sub>2</sub>O<sub>2</sub> dosage variation perpendicular lines were in the range of 2.0 to 2.34 ml/L. Similarly, the removal rate had little change and then decreased slightly with the H<sub>2</sub>O<sub>2</sub> dosage from 1.0 to 1.02 ml/L and increasing catalyst dosage. The removal rate was increased to 94% by increasing the catalyst dosage. And then the removal rate was decreased slightly by increasing H<sub>2</sub>O<sub>2</sub> dosage from 1.02 to 2.68 ml/L. Furthermore, the H<sub>2</sub>O<sub>2</sub> dosage was increased to 3.0 ml/L, the removal rate was first increased and then remained constant. When the H<sub>2</sub>O<sub>2</sub> dosage was constant, the six tangent points of different contour lines and catalyst dosage variation horizontal lines were in the range of 0.80–1.22 g/L. The removal rate became decreased with the low catalyst dosage (0.5–0.7 g/L) and the low H<sub>2</sub>O<sub>2</sub> dosage (1.0–1.5 ml/L). On the whole, the interaction between the H<sub>2</sub>O<sub>2</sub> dosage and the catalyst dosage would be obvious with the large extreme point deviation. When H<sub>2</sub>O<sub>2</sub> dosage was 2.04–2.24 ml/L and the catalyst dosage was 0.92–1.18 g/L, the removal rate of Reactive Red X-3B (2,000 mg/L) was 94%.

All quadratic terms of RSM were significant. The catalyst dosage and the substrate concentration also had

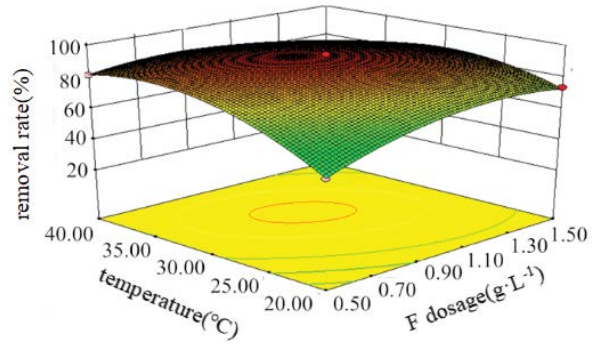
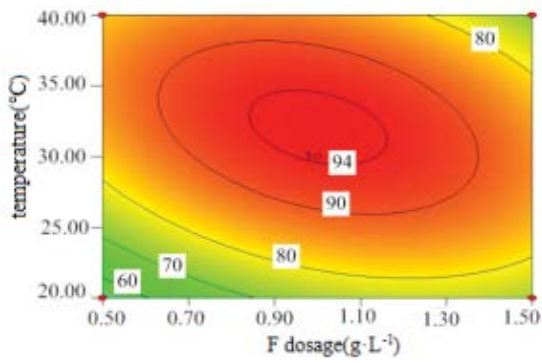
interactions. Substrate concentration had a negative quadratic effect on the reaction. The removal rate was decreased with high substrate concentration. The interaction between substrate concentration and catalyst dosage had shown in Fig. 4c. Thereafter, the removal rate was increased with the unchanged substrate concentration. And then the removal rate was decreased slightly with increasing catalyst dosage. It was shown that the seven tangent points of different contour lines and catalyst dosage variation horizontal lines were in the range of 0.98–1.10 g/L. Similarly, the removal rate had increased and then decreased slightly with increasing substrate concentration. The four tangent points of different contour lines and substrate concentration variation perpendicular lines were in the range of 1,625–1,750 mg/L. Finally, the extreme value indicated that the interaction between substrate concentration and catalyst dosage was small.

RSM was used to predict the optimum conditions of photocatalytic degradation of Reactive Red X-3B by F. The predicted removal rate of Reactive Red X-3B was 100% when the following optimum conditions were used: F dosage of 0.98 g/L, H<sub>2</sub>O<sub>2</sub> dosage of 2.33 ml/L, the Reactive Red X-3B concentration of 1,626 mg/L, and the temperature of 30.6°C. The deviation value between the experimental result and the predicted value was 1.72%. The results were indicated that the fitting effects of the model were good.

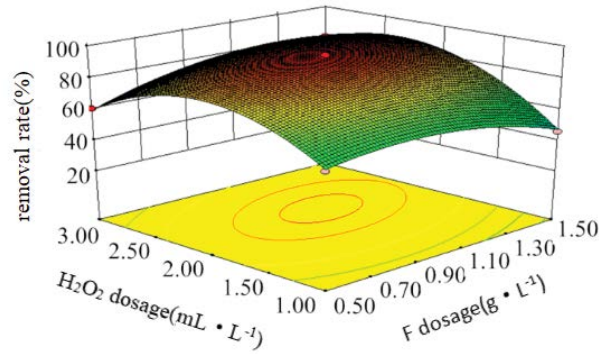
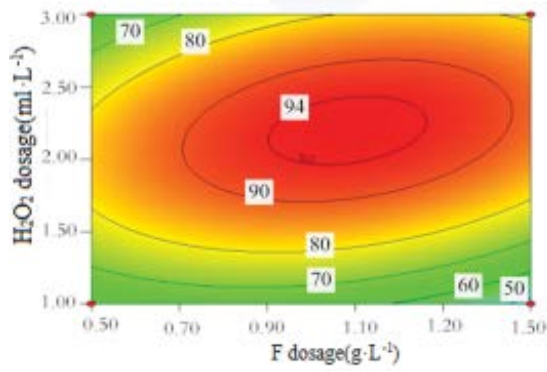
### 3.3. Response surfaces model fittings of molecular sieve Ti/F

Tables 6 and 7 show the statistical analysis about the model of Reactive Red X-3B by Ti/F. As the results in Table 6, the analysis of F accorded with quadratic equation by sequential *p*-value (<0.0001) and the “lack of fit” of 0.0501. The results indicated that the model terms were significant.

(a)



(b)



(c)

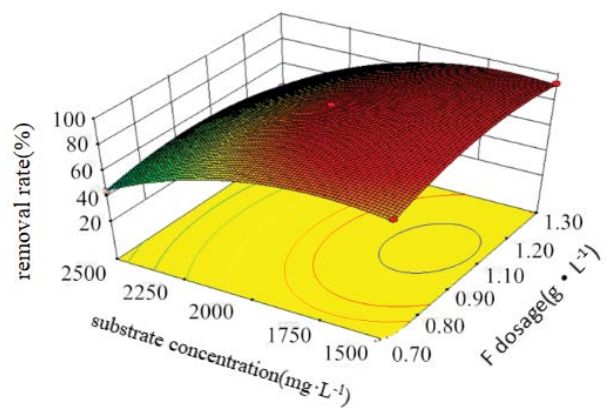
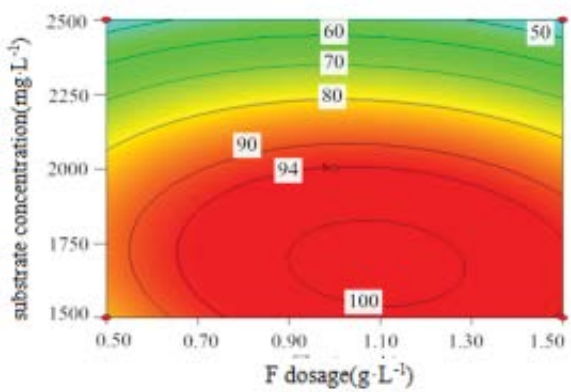


Fig. 4. 3-Dimensional response surface plots showing the effects of interaction of F. (a) Model graph of the interaction A and D variable, (b) model graph of the interaction A and C variable, and (c) model graph of the interaction A and B variable.

Table 6  
Statistical analysis for Ti/F of response surface model fitting

Source	Sequential <i>p</i> -value	Lack of fit <i>p</i> -value	Adj. <i>R</i> -Squared	Pred. <i>R</i> -Squared
Linear	0.0015	0.0038	0.4235	0.3439
2FI	0.6661	0.0029	0.3738	0.1728
Quadratic	<0.0001	0.0501	0.8668	0.6277
Cubic	0.2391	0.0468	0.9096	−1.2308

Table 7  
Variance analysis of Box–Behnken experimental design

Source	Sum of squares	df	Mean square	<i>F</i> -value	<i>p</i> -value Prob. > <i>F</i>	
Model	10,449.9	14	746.42	14.02	<0.0001	Extremely significant
<i>A</i>	150.52	1	150.52	2.83	0.1149	
<i>B</i>	4,603.65	1	4,603.65	86.45	<0.0001	
<i>C</i>	694.18	1	694.18	13.04	0.0028	
<i>D</i>	215.31	1	215.31	4.04	0.0640	
<i>AB</i>	14.94	1	14.94	0.28	0.6047	
<i>AC</i>	5.04	1	5.04	0.095	0.7629	
<i>AD</i>	705.43	1	705.43	13.25	0.0027	
<i>BC</i>	64.8	1	64.8	1.22	0.2886	
<i>BD</i>	141.73	1	141.73	2.66	0.1251	
<i>CD</i>	93.12	1	93.12	1.75	0.2072	
<i>A</i> <sup>2</sup>	1,221.02	1	1,221.02	22.93	0.0003	
<i>B</i> <sup>2</sup>	1,171.26	1	1,171.26	21.99	0.0003	
<i>C</i> <sup>2</sup>	2,654.96	1	2,654.96	49.86	<0.0001	
<i>D</i> <sup>2</sup>	229.93	1	229.93	4.32	0.0566	
Residual	745.51	14	53.25			
Lack of fit	698.58	10	69.86	5.95	0.0501	Not significant
Pure error	46.93	4	11.73			
Cor. total	11,195.42	28				

Further statistical analyses with standard deviation and mean showed that the “Pred. *R*-Squared” of 0.6277 was in reasonable agreement with the “Adj. *R*-Squared” of 0.8668. The results implied that the removal rates of Reactive Red X-3B by molecular sieve Ti/F were fitted to the following quadratic model.

$$R_2 = 96.02 - 3.54A - 19.59B + 7.61C + 4.24D + 1.93AB - 1.12AC - 13.28AD - 4.03BC + 5.59BD - 4.82CD - 13.72A^2 - 13.44B^2 - 20.23C^2 - 5.59D^2 \quad (5)$$

where *R*<sup>2</sup>: removal rate (%); *A*: code value of catalyst dosage; *B*: code value of substrate concentration; *C*: code value of H<sub>2</sub>O<sub>2</sub> dosage; *D*: code value of temperature.

Therefore, the model was navigated in the design space. Similar conclusion had been reported by Khorram and Fallah [40] that the significance of each coefficient of the response equation was determined by *p*-value.

The effects of catalyst dosage, the dosage of H<sub>2</sub>O<sub>2</sub>, substrate concentration, and reaction temperature were all significant with coefficients (Supplementary information). The temperature had the largest effect. The higher temperature

promoted the degradation of Reactive Red X-3B. The removal rate was increased with the temperature from 20°C to 30°C; however, the removal rate was constant at over 30°C. Increasing catalyst dosages showed a less pronounced effect on the removal rate. A small positive effect was seen with the catalyst dosage over 0.4 g/L. Furthermore, the temperature and the catalyst dosage had a significantly positive interaction. The removal rate was further increased with simultaneously small or large parameter values. However, the effects and the strong positive interaction with temperature dominated the RSM plot of temperature and catalyst dosage (Fig. 5a). The removal rate was basically unchanged with the temperature of 20°C–22°C and increasing catalyst dosage. The removal rate raised to 94% with increasing catalyst dosage at 38°C and then decreased. The removal rate was 90%–96% with the temperature at 22°C–30°C. Therefore, the removal rate had been increased to the maximum (96%) at 38°C. Similarly, the removal rate had little change and then decreased slightly with catalyst dosage increased at 38°C–40°C. Also, the removal rate gradually increased and then tended to remain unchanged by increasing temperature and the catalyst dosage was 0.5–0.94 g/L. Similarly, when catalyst dosage was 0.94–1.28 g/L, the removal rate

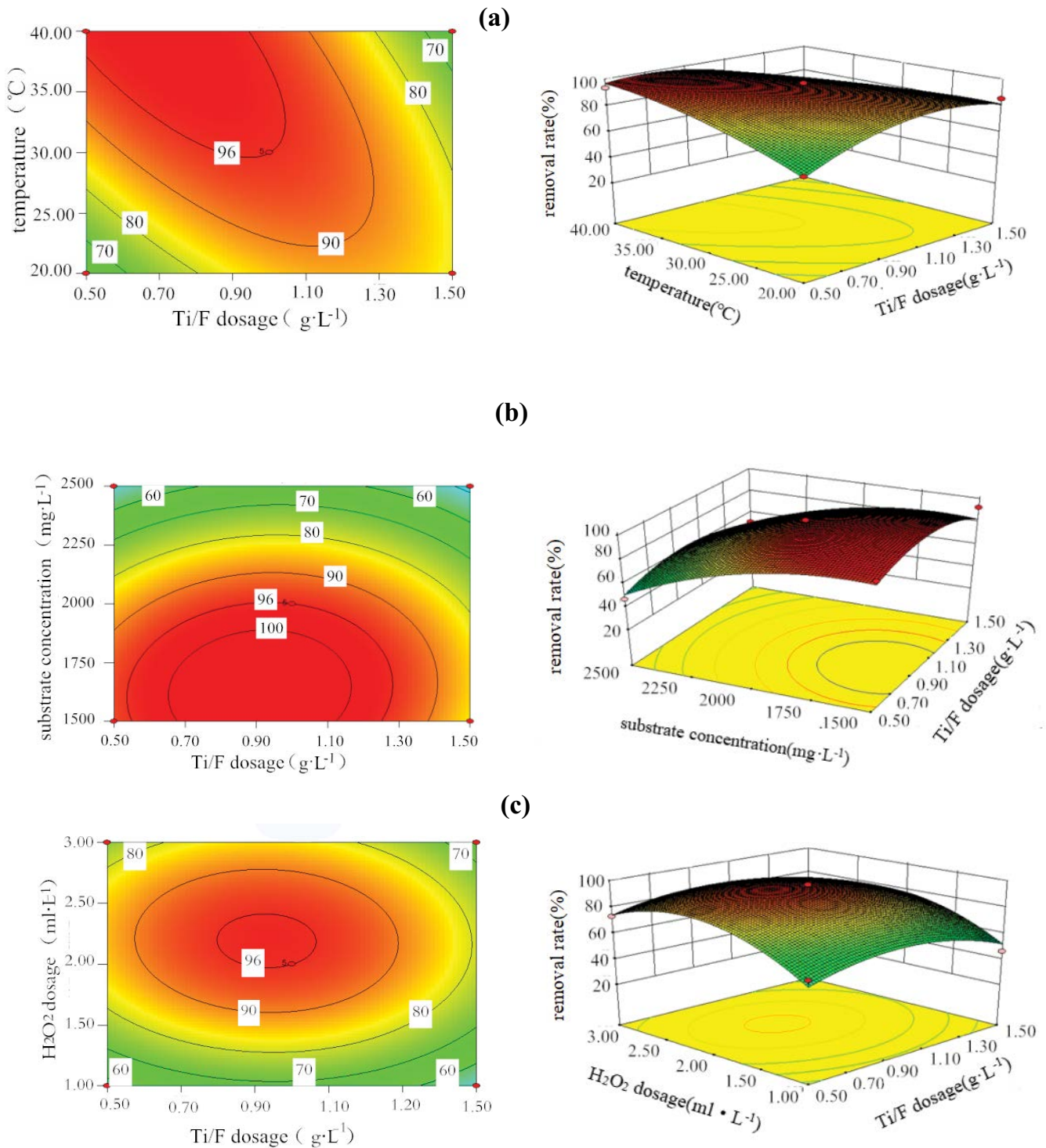


Fig. 5. 3-Dimensional response surface plots showing the effects of interaction of Ti/F. (a) Model graph of the interaction A and D variable, (b) model graph of the interaction A and B variable, and (c) model graph of the interaction A and C variable.

increased first and then decreased by increasing temperature. The removal rate first remained unchanged and then decreased by increasing temperature with the catalyst dosage was 0.94–1.28 g/L. The effects of temperature and catalyst dosage on the removal rate were positive. The tangent point of the horizontal line at constant temperature and the

tangent point of the vertical line at constant catalyst dosage had big deviations with two temperature contour lines (96% and 90%). It was included that the temperature and the catalyst dosage had interaction.

Substrate concentration had a negative quadratic effect, that is, the removal rate had decreased with high substrate

concentration. The interaction between substrate concentration and catalyst dosage is shown in Fig. 5b. When the dosage of  $H_2O_2$  was constant, the removal rate of Reactive Red X-3B was basically constant and then gradually decreased with increasing substrate concentration, while the conditions were 30°C and 1.0 g/L Ti/F. The removal rate was decreased after increasing to the maximum with the catalyst dosage of 0.68–1.12 g/L and increasing substrate concentration. The removal rate was increased and then decreased with increasing substrate concentration, whether the catalyst dosage was smaller than 0.68 g/L or larger than 1.12 g/L. The tangent point of the vertical line with constant catalyst dosage and the tangent point of the horizontal line with temperature constant had a small deviation. It was shown the interaction between the catalytic dose and the substrate concentration was minimal. The contour was shown that the removal rate was 100%. The contour included that the removal rate of 100% with the substrate concentration of 1,887 mg/L and catalyst dosage of 0.92 g/L. When the catalyst dosage was 0.80–1.03 g/L and substrate concentration was 1,500–1,870 mg/L, the removal rate of Reactive Red X-3B (2,000 mg/L) was 100%.

The  $H_2O_2$  dosage showed a less pronounced effect on the removal rate than temperature and substrate concentration. The  $H_2O_2$  inhibited the reaction when the dosage above 2 ml/L. A small though the positive effect was seen from  $H_2O_2$  dosage under 2 ml/L. Furthermore,  $H_2O_2$  dosage had a significant positive and negative interactions with each factor. The effects and strong interaction with  $H_2O_2$  dosage are shown in RSM (Fig. 5c). When the dosage of Ti/F was constant, the removal rate of Reactive Red X-3B was increased first and then decreased with increasing  $H_2O_2$  dosage. Similarly, when the  $H_2O_2$  dosage was constant, the removal rate of Reactive Red X-3B was increased first and then decreased with increasing the catalyst dosage continuously. On the whole, the tangent point of the horizontal line with constant  $H_2O_2$  dosage and the tangent point of the vertical line with constant catalyst dosage had little deviation. It included that the  $H_2O_2$  dosage and the catalyst dosage had interaction.

RSM was used to predict the optimum conditions of photocatalytic degradation of Reactive Red X-3B by F. The predicted removal rate of Reactive Red X-3B was 100% when the following optimum conditions were used: Ti/F dosage of 0.80 g/L,  $H_2O_2$  dosage of 2.01 ml/L, the Reactive Red X-3B concentration of 1,824 mg/L and the temperature of 32.5°C. The deviation value between the experimental result and the predicted value was 2.17%. The results were indicated that the fitting effects of the model were good.

#### 4. Conclusion

This study investigated the effects of the two most important molecular sieves on catalyzing the degradation of Reactive Red X-3B. A systematic approach was used to optimize the reaction condition and to fit a quadratic model. The RSM was used to account for the effect on the factors of molecular sieves, catalyst dosage,  $H_2O_2$  dosage, substrate concentration of Reactive Red X-3B, and reaction temperature. The different molecular sieves were used as effective catalysts for dealing with dye wastewater. In conclusion, the feasibility of the molecular sieve to deal with Reactive Red X-3B was confirmed. The results showed that the optimum

conditions of the maximum Reactive Red X-3B removal with 98.28% by molecular sieve F: catalyst dosage of 0.98 g/L, an initial Reactive Red X-3B concentration of 1,626 mg/L, a temperature of 30.6°C and  $H_2O_2$  dosage of 2.33 ml/L. The removal rate of the maximum Reactive Red X-3B was 97.83% by molecular sieve Ti/F under optimum conditions: catalyst dosage of 0.80 g/L, an initial Reactive Red X-3B concentration of 1,824 mg/L, a temperature of 32.5°C and  $H_2O_2$  dosage of 2.01 ml/L.

#### Acknowledgments

This work was supported by the National Key Technology R&D Program (2017YFD0300503) and the Applied Basic Research Programs of Science and Technology Commission Foundation of Heilongjiang Province (No.GC13B111)

#### References

- [1] I. Mohmood, C.B. Lopes, I. Lopes, I. Ahmad, A.C. Duarte, E. Pereira, Nanoscale materials and their use in water contaminants removal—a review, *Environ. Sci. Pollut. Res.*, 20 (2013) 1239–1260.
- [2] S. Naidoo, A.O. Olaniran, Treated wastewater effluent as a source of microbial pollution of surface water resources, *Int. J. Environ. Res. Public Health*, 11 (2014) 249–270.
- [3] L. Tan, S.X. Ning, X.W. Zhang, S.N. Shi, Aerobic decolorization and degradation of azo dyes by growing cells of a newly isolated yeast *Candida tropicalis* TL-F1, *Bioresour. Technol.*, 138 (2013) 307–313.
- [4] E. Bizani, K. Fytianos, I. Poullos, V. Tsiridis, Photocatalytic decolorization and degradation of dye solutions and wastewaters in the presence of titanium dioxide, *J. Hazard. Mater.*, 136 (2006) 85–94.
- [5] Z.P. Cao, J.H. Zhang, J.L. Zhang, H.W. Zhang, Degradation pathway and mechanism of Reactive Brilliant Red X-3B in electro-assisted microbial system under anaerobic condition, *J. Hazard. Mater.*, 329 (2017) 159–165.
- [6] S.S. Swati, A.N. Faruqi, Investigation on ecological parameters and COD minimization of textile effluent generated after dyeing with mono and bi-functional reactive dyes, *Environ. Technol. Innovation*, 11 (2018) 165–173.
- [7] J. Wang, Y.N. Yan, L.L. Tian, Q.M. Wang, Y. Zhang, W.Q. Cao, C. Yang, Efficient electrochemical oxidation of charged cryogel adsorbed reactive dyes in non-aqueous media, *Water Air Soil Pollut.*, 229 (2018) 180, <https://doi.org/10.1007/s11270-018-3833-y>.
- [8] R.D. Saini, Textile organic dyes: polluting effects and elimination methods from textile waste water, *Int. J. Eng. Sci.*, 9 (2017) 121–136.
- [9] C.M. So, M.Y. Cheng, J.C. Yu, P.K. Wong, Degradation of azo dye Procion Red MX-5B by photocatalytic oxidation, *Chemosphere*, 46 (2002) 905–912.
- [10] J. Grzechulska, A.W. Morawski, Photocatalytic decomposition of azo-dye acid black 1 in water over modified titanium dioxide, *Appl. Catal., B*, 36 (2002) 45–51.
- [11] S.C. Kwon, M.H. Fan, A.T. Cooper, H.Q. Yang, Photocatalytic applications of micro- and nano-TiO<sub>2</sub> in environmental engineering, *Crit. Rev. Env. Sci. Technol.*, 38 (2008) 197–226.
- [12] K.M. Reza, A.S.W. Kurny, F. Gulshan, Parameters affecting the photocatalytic degradation of dyes using TiO<sub>2</sub>: a review, *Appl. Water Sci.*, 7 (2017) 1569–1578.
- [13] M.Y. Ghaly, T.S. Jamil, I.E. El-Seesy, E.R. Souaya, R.A. Nasr, Treatment of highly polluted paper mill wastewater by solar photocatalytic oxidation with synthesized nano-TiO<sub>2</sub>, *Chem. Eng. J.*, 168 (2011) 446–454.
- [14] A. Zaleska, Doped-TiO<sub>2</sub>: a review, *Recent Pat. Eng.*, 2 (2008) 157–164.
- [15] A.R. Khataee, V. Vatanpour, A.R. Amani Ghadim, Decolorization of C.I. Acid Blue 9 solution by UV/Nano-TiO<sub>2</sub>, Fenton,

- Fenton-like, electro-Fenton and electrocoagulation processes: a comparative study, *J. Hazard. Mater.*, 161 (2009) 1225–1233.
- [16] Y. Kuwahara, T. Kamegawa, K. Mori, H. Yamashita, Design of new functional titanium oxide-based photocatalysts for degradation of organics diluted in water and air, *Curr. Org. Chem.*, 14 (2010) 616–629.
- [17] N. Taoufik, A. Elmchaouri, F. Anouar, S.A. Korili, A. Gil, Improvement of the adsorption properties of an activated carbon coated by titanium dioxide for the removal of emerging contaminants, *J. Water Process Eng.*, 31 (2019) 100876, <https://doi.org/10.1016/j.jwpe.2019.100876>.
- [18] D.M. Chen, Q. Zhu, F.S. Zhou, X.T. Deng, F.T. Li, Synthesis and photocatalytic performances of the TiO<sub>2</sub> pillared montmorillonite, *J. Hazard. Mater.*, 235 (2012) 186–193.
- [19] K. Ikeue, H. Yamashita, M. Anpo, T. Takekawa, Photocatalytic reduction of CO<sub>2</sub> with H<sub>2</sub>O on Ti-β zeolite photocatalysts: effect of the hydrophobic and hydrophilic properties, *J. Phys. Chem., B*, 105 (2001) 8350–8355.
- [20] M.A. Fox, K.E. Doan, M.T. Dulay, The effect of the “Inert” support on relative photocatalytic activity in the oxidative decomposition of alcohols on irradiated titanium dioxide composites, *Res. Chem. Intermed.*, 20 (1994) 711, <https://doi.org/10.1163/156856794X00504>.
- [21] Y.J. Li, X.D. Li, J.W. Li, J. Yin, Photocatalytic degradation of methyl orange by TiO<sub>2</sub>-coated activated carbon and kinetic study, *Water Res.*, 40 (2006) 1119–1126.
- [22] J.-H. Sun, Y.-K. Wang, R.-X. Sun, S.-Y. Dong, Photodegradation of azo dye Congo Red from aqueous solution by the WO<sub>3</sub>-TiO<sub>2</sub>/activated carbon (AC) photocatalyst under the UV irradiation, *Mater. Chem. Phys.*, 115 (2009) 303–308.
- [23] M. Asiltürk, S. Şener, TiO<sub>2</sub>-activated carbon photocatalysts: preparation, characterization and photocatalytic activities, *Chem. Eng. J.*, 180 (2012) 354–363.
- [24] R.J. Tayade, R.G. Kulkarni, R.V. Jasra, Enhanced photocatalytic activity of TiO<sub>2</sub>-coated NaY and HY zeolites for the degradation of methylene blue in water, *Ind. Eng. Chem. Res.*, 46 (2007) 369–376.
- [25] S.F. Chen, Y.Z. Liu, Study on the photocatalytic degradation of glyphosate by TiO<sub>2</sub> photocatalyst, *Chemosphere*, 67 (2007) 1010–1017.
- [26] M.V. Bosco, M. Garrido, M.S. Larrechi, Determination of phenol in the presence of its principal degradation products in water during a TiO<sub>2</sub>-photocatalytic degradation process by three-dimensional excitation–emission matrix fluorescence and parallel factor analysis, *Anal. Chim. Acta*, 559 (2006) 240–247.
- [27] A. Witek-Krowiak, K. Chojnacka, D. Podstawczyk, A. Dawiec, K. Pokomeda, Application of response surface methodology and artificial neural network methods in modelling and optimization of biosorption process, *Bioresour. Technol.*, 160 (2014) 150–160.
- [28] Y.H. Tan, M.O. Abdullah, C. Nolasco-Hipolito, N.S.A. Zauzi, Application of RSM and Taguchi methods for optimizing the transesterification of waste cooking oil catalyzed by solid ostrich and chicken-eggshell derived CaO, *Renewable Energy*, 114 (2017) 437–447.
- [29] J.A. Pinto, M.A. Prieto, I.C.F.R. Ferreira, M.N. Belgacem, A.E. Rodrigues, M.F. Barreiro, Analysis of the oxypropylation process of a lignocellulosic material, almond shell, using the response surface methodology (RSM), *Ind. Crops Prod.*, 153 (2020) 112542, <https://doi.org/10.1016/j.indcrop.2020.112542>.
- [30] M.A. Bezerra, R.E. Santelli, E.P. Oliveira, L.S. Villar, L.A. Escalera, Response surface methodology (RSM) as a tool for optimization in analytical chemistry, *Talanta*, 76 (2008) 965–977.
- [31] U. Natarajan, P.R. Periyanan, S.H. Yang, Multiple-response optimization for micro-endmilling process using response surface methodology, *Int. J. Adv. Manuf. Technol.*, 56 (2011) 177–185.
- [32] S. Daneshgar, P.A. Vanrolleghem, C. Vaneekhaute, A. Buttafava, A.G. Capodaglio, Optimization of P compounds recovery from aerobic sludge by chemical modeling and response surface methodology combination, *Sci. Total Environ.*, 668 (2019) 668–677.
- [33] G.J. Swamy, A. Sangamithra, V. Chandrasekar, Response surface modeling and process optimization of aqueous extraction of natural pigments from *Beta vulgaris* using Box–Behnken design of experiments, *Dyes Pigm.*, 111 (2014) 64–74.
- [34] R.H. Myers, D.C. Montgomery, C.M. Anderson-Cook, *Response Surface Methodology: Process and Product Optimization Using Designed Experiments*, JWA, America, 2016.
- [35] F. Geyikçi, E. Kılıç, S. Çoruh, S. Elevli, Modelling of lead adsorption from industrial sludge leachate on red mud by using RSM and ANN, *Chem. Eng. J.*, 183 (2012) 53–59.
- [36] M. Boumaaza, A. Belaadi, M. Bourchak, The effect of alkaline treatment on mechanical performance of natural fibers-reinforced plaster: optimization using RSM, *J. Nat. Fibers* (2020) 1–21, <https://doi.org/10.1080/15440478.2020.1724236>.
- [37] X.K. Li, L.X. Yang, Y. Zhang, W.J. Zhang, Polyethylene glycol in sol-gel precursor to prepare porous Gd<sub>2</sub>Ti<sub>2</sub>O<sub>7</sub>: enhanced photocatalytic activity on Reactive Brilliant Red X-3B degradation, *Mater. Sci. Semicond. Process.*, 117 (2020) 105181, <https://doi.org/10.1016/j.mssp.2020.105181>.
- [38] H. Deng, Y.H. Wang, X.C. Zhang, X.Q. Kou, B. Chen, C.C. Zhu, Photodegradation under natural indoor weak light assisted adsorption of X-3B on TiO<sub>2</sub>/Al<sub>2</sub>O<sub>3</sub> nanocomposite, *Chem. Eng. J.*, 372 (2019) 99–106.
- [39] V. Kumar, P. Saharan, A.K. Sharma, A. Umar, I. Kaushal, A. Mittal, Y. Al-Hadeethi, B. Rashad, Silver doped manganese oxide-carbon nanotube nanocomposite for enhanced dye-sequestration: isotherm studies and RSM modelling approach, *Ceram. Int.*, 54 (2020) 109–116.
- [40] A.G. Khorram, N. Fallah, Treatment of textile dyeing factory wastewater by electrocoagulation with low sludge settling time: optimization of operating parameters by RSM, *J. Environ. Eng.*, 6 (2018) 635–642.

## Supporting information

### S1. Characterization of F and Ti/F

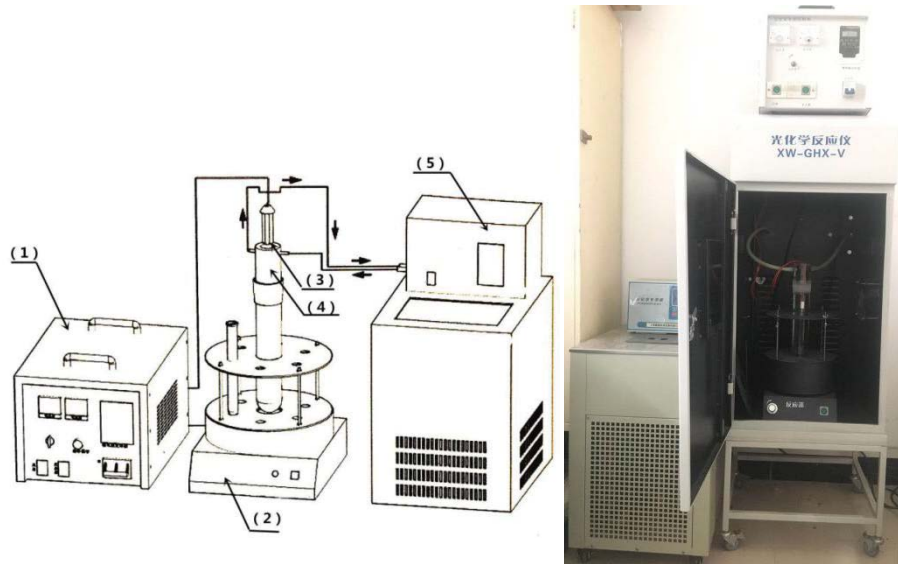
The morphologies of F, Ti/F composites were observed by field-emission scanning electron microscopy, as depicted in Table 1. Pristine F displayed a typically aggregated morphology with a number of block-based particles. F exhibited flower-like hierarchical microspheres with an average pore size at 26.59 nm. It was noted that there were many small irregular pores appeared on the surface, which could be ascribed to the fact that a large amount of small molecule was released during removal. After loading TiO<sub>2</sub>, Ti/F maintained thin-sheet structures with the pores, which might decrease the surface area. Besides, because of the excessive stomata on the surface of the nano-sheets, the removal efficiency was significantly improved.

Furthermore, the introduction of TiO<sub>2</sub> additives in F can also be demonstrated using energy-dispersive X-ray spectroscopy (EDS) and the corresponding EDS patterns shown in Table 1. EDS analysis indicated that the TiO<sub>2</sub> was successfully embedded into F by the hydrothermal synthesis method. Hence, it is shown that O, C, Si, Al, Na elements were detected using EDS in all samples, which ascribed to their high content. SiO<sub>2</sub>, Al<sub>2</sub>O<sub>3</sub>, Na<sub>2</sub>O were the main oxide compositions of fly ash and NaOH melting calcination. In addition, the embedding of TiO<sub>2</sub> in F not only increased the number of Ti but also caused the number of Ca, Fe, Cu decreased during loading TiO<sub>2</sub>, Ti ion-exchange replaced them.

The specific surface areas of F and Ti/F are 24.11 and 10.91 m<sup>2</sup>/g, respectively (Fig. 1). Reactive Red X-3B can be effectively adsorbed by F and Ti/F. The numbers of specific

surface area, total pore volume and micropore volume of F are bigger than Ti/F. It indicated that the surface structure of molecular sieve F was changed during the process of loading TiO<sub>2</sub>. Moreover, the total pore volume of Ti/F has been small, which is due to the sticky structure of Ti blocked the original voids of the molecular sieve F.

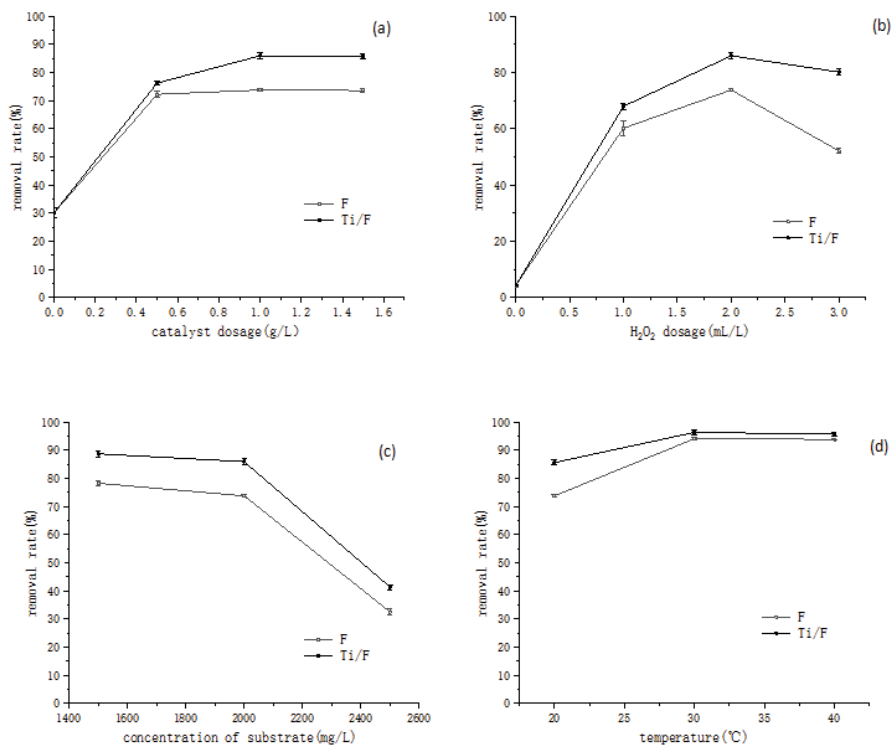
S2. Experimental arrangement



(1) Lighting controller; (2) magnetic stirring apparatus; (3) light source; (4) quartz water cooling tube; (5) low-temperature thermostat bath.

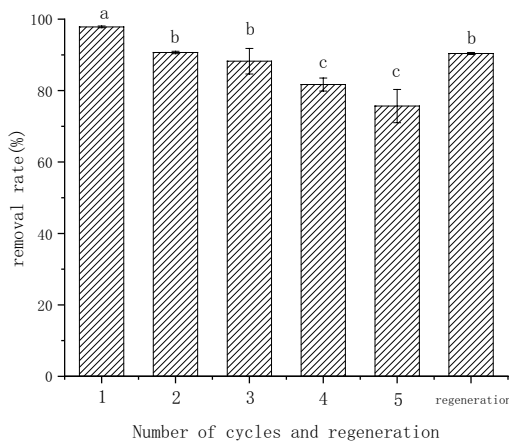
The equipment has to light controller, magnetic stirring apparatus light source quartz water cooling tube and low-temperature thermostat bath. The experimental arrangement was used to provide UV.

S3. Single-factor test



The effects of catalyst dosage,  $H_2O_2$  dosage, concentration substrate and reaction temperature were shown in the figure. The removal rate was increasing with increasing catalyst dosage. A small though the positive effect is seen from  $H_2O_2$  dosage under 2 ml/L, however, the  $H_2O_2$  dosage above 2 ml/L may simply lead to Reactive Red X-3B degradation being inhibited. The removal rate was reduced by increasing the concentration of substrate. And the temperature promoted degradation.

#### S4. Results of catalyst cycle times and regeneration test



There is no denying that stability and reusability were important parameters for photocatalysts in the application of wastewater treatment. Thus, in order to evaluate the stability and reusability of Ti/F, which habited the high recyclable reuse performance was achieved by calcination at 450°C for 1.5 h. The by-products of photocatalytic reaction have accumulated with increasing the cycle reaction times, which hindered the progress and had reduced the photocatalytic activity. The removal rate of Ti/F was 90.39% after a consecutive 5 recycling run, suggesting that it has prominent reusability. Moreover, the good stability and reusability of Ti/F photocatalyst further indicated that this system could be applied as a promising candidate for wastewater treatment.